

# Semi-Static Radio Frame Configuration for URLLC Deployments in 5G Macro TDD Networks

Ali A. Esswie<sup>1,2</sup>, Klaus I. Pedersen<sup>1,2</sup>, and Preben E. Mogensen<sup>1,2</sup>

<sup>1</sup>Nokia Bell-Labs, Aalborg, Denmark

<sup>2</sup>Department of Electronic Systems, Aalborg University, Denmark

**Abstract**—Dynamic time division duplexing (TDD) is one of the major novelties of the 5G new radio standard. It notably improves the network resource utilization with sporadic directional packet arrivals. Although, the feasibility of the ultra-reliable and low-latency communications (URLLC) within such deployments is critically challenged, mainly due to the cross-link interference (CLI). In this work, we propose a semi-static and computationally-efficient TDD radio frame adaptation algorithm for 5G macro deployments. Particularly, we first identify the quasi-static variance of the cross-cell traffic buffering performance, with various CLI co-existence conditions. Accordingly, a common radio frame pattern is dynamically estimated based on the filtered multi-cell traffic statistics. Our system-level simulation results show that the proposed solution achieves a highly improved URLLC outage performance, i.e., offering  $\sim 40\%$  reduction gain of the achievable URLLC outage latency compared to perfect static-TDD, and approaching the optimal interference-free flexible-TDD case; though, with a significantly lower control overhead size.

**Index Terms**— Dynamic TDD; 5G new radio; URLLC; Traffic; Cross link interference (CLI).

## I. INTRODUCTION

Ultra-reliable and low latency communication (URLLC) is the major service class of the upcoming fifth generation new radio (5G-NR) standards [1], where it enables a new set of cutting-edge and real-time applications over wireless mediums, e.g., interactive tactile-internet. URLLC entails sporadic radio transmissions of a small payload size, with stringent radio latency and reliability targets of one-way radio latency of 1 millisecond with a 99.999% success probability [2]. Most of the 5G-NR deployments are envisioned to be with the time division duplexing (TDD) due to its large spectrum availability [3]. Achieving the URLLC targets are particularly challenging for TDD systems [4] because of: (a) the non-concurrent downlink (DL) and uplink (UL) transmission opportunities, and (b) additional cross-link interference (CLI) among neighboring base-stations (BSs) adopting opposite transmission directions. Those challenges are particularly non-trivial for wide-area macro deployments and are the focus of this paper.

The 5G-NR has defined a flexible slot format design [5], where the TDD adaptation periodicity can be slot-based, i.e., in principal, per every 14 orthogonal frequency division multiplexing (OFDM) symbols. Thus, the DL/UL link switching delay is minimized down to less than a millisecond. However, the CLI still remains a critical capacity limitation of the flexible TDD deployments. In particular, for a macro setting, the DL-to-UL CLI, i.e., BS-BS CLI, is most problematic due to

the power imbalance between the DL interfering transmissions and the UL victim receptions.

In this study, we focus on achieving the URLLC-alike requirements for macro deployments at frequency range one (FR1), i.e. radio frequency (RF) operation below 7 GHz. For FR1, neighboring spectrum chunks are expected to be allocated for different operators. Accordingly, inter-operator co-existence must be considered, especially to handle the TDD inter-frequency interference. A study of the 5G-NR TDD RF co-existence was recently completed by 3GPP, concluding that fully-flexible and uncoordinated TDD deployments are not possible for FR1 macro deployments due to the severe BS-BS CLI [6], hence, recommending that operators must adopt fully-aligned TDD radio frame configurations (RFCs) to avoid the harmful inter-frequency CLI.

Furthermore, even for single-operator cases, co-channel CLI has been identified as a severe problem for macro deployments, leading the use of fully-dynamic TDD to be further challenging. Various methods to partially handle the co-channel CLI problem have therefore been proposed in the open literature. Those include CLI cancellation techniques [7-10] through inter-cell coordinated user scheduling, joint transceiver design, power control, and beam-forming. Simpler quasi-dynamic and opportunistic CLI avoidance schemes are also introduced based on hybrid RFC design [11-13]. However, although those techniques offer performance gain, the CLI problem remains non-negligible, and particularly harmful for URLLC use cases due to the strict requirements of the achievable latency and reliability. Needles to say, a simpler, overhead-limited and CLI-free adaptive RFC selection algorithm is still vital for 5G macro TDD deployments.

In this paper, a semi-static and fully-aligned RFC selection algorithm is proposed for 5G-NR TDD networks. Proposed solution offers CLI-free TDD transmissions while semi-statically adjusting the RFCs to manage the tail of the latency-reliability distribution of the experienced user performance, as the primary performance indicator for URLLC use cases. The cell-specific traffic load metrics are exchanged across coordinating cells, and are filtered to either adapt the upcoming RFCs to the average or individual cell outage performance. Hence, the proposed solution adaptively controls the tail distribution of the cluster capacity and latency, which contributes towards achieving a decent URLLC outage latency. As the RFC selection is NP-hard problem for multi-user URLLC deployments, we evaluate the performance of the proposed solution by means extensive dynamic system-level simulations to achieve results

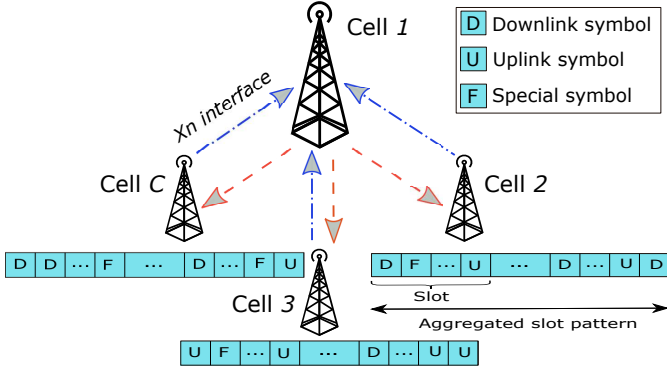


Fig. 1. Flexible-TDD network deployment.

with high degree of realism. That is, we consider a dynamic multi-cell, multi-user environment in line with the 5G-NR specifications, and following the 3GPP simulation modeling guidelines, e.g. relying on advanced stochastic models for radio propagation, traffic generation, etc.). Care is taken to achieve trustworthy and statistical-reliable performance results as a basis for drawing conclusions.

This paper is organized as follows. Section II presents our system setting. Section III discusses the problem formulation addressed by this work, while Section IV introduces the proposed scheme. The performance evaluation appears in Section V. Finally, conclusions are drawn in Section VI.

## II. SYSTEM MODEL

We assume a macro 5G-NR TDD network deployment, with  $C$  cells, each with  $N_t$  antennas. There exists an average number of  $K^{\text{dl}}$  and  $K^{\text{ul}}$  uniformly-distributed DL and UL active user-equipment's (UEs) per cell, each equipped with  $M_r$  antennas. Herein, we consider the FTP3 traffic model with payload sizes  $f^{\text{dl}}$  and  $f^{\text{ul}}$  bits, and Poisson Point Arrival Process, with mean packet arrivals  $\lambda^{\text{dl}}$  and  $\lambda^{\text{ul}}$ , for DL/UL links. Hence, the total offered average load per cell is given as:  $\Omega = \Omega^{\text{dl}} + \Omega^{\text{ul}}$ , with  $\Omega^{\text{dl}} = K^{\text{dl}} \times f^{\text{dl}} \times \lambda^{\text{dl}}$ , and  $\Omega^{\text{ul}} = K^{\text{ul}} \times f^{\text{ul}} \times \lambda^{\text{ul}}$  as the average DL and UL offered load sizes, respectively.

We follow the latest 3GPP specifications for the 5G-NR TDD system design. Particularly, the 5G-NR flexible TDD slot format structure [5] is considered, as depicted by Fig. 1. A slot format implies a certain placement of DL [D], UL [U] and flexible [F] symbols each 14-OFDM slot duration. In this work, we assume an even distribution of the DL and UL symbols over the slot in terms of a 4-symbol block size. For instance, a selected slot format with a DL:UL symbol ratio of 2 : 1 would be: **[DDDDFUUUUDDDDDF]**. This configuration allows for sparse DL and UL transmission opportunities during a slot; though, at the expense of increased guard overhead, i.e., [F] symbols. During each slot, UEs are dynamically multiplexed using the OFDM access (OFDMA), with 30 kHz sub-carrier-spacing (SCS) and a physical resource block (PRB) of 12 consecutive SCs. The dynamic user scheduling is performed based on the proportional fair (PF) criterion, and with a transmit time interval (TTI) duration of 4-OFDM symbols, for rapid URLLC radio transmissions. The achievable one-way outage URLLC latency is the main performance indicator

of this work. It encompasses the delay from the moment the URLLC packet becomes available at the packet data convergence protocol (PDCP) layer until it has been successfully decoded, including the BS and UE processing delay, hybrid automatic repeat request (HARQ) re-transmission delay, and scheduling buffering delay, respectively, in line with [4]. For UL transmissions, we assume a fast dynamic grant (DG) [4], where the UL packets become immediately available for scheduling upon availability at the UE PDCP layer. That is, the time from transmitting the UL scheduling request until receiving the DL scheduling grant is assumed negligible.

Lets define  $\mathfrak{B}_{\text{dl}}$ ,  $\mathfrak{B}_{\text{ul}}$ ,  $\mathcal{K}_{\text{dl}}$  and  $\mathcal{K}_{\text{ul}}$  as the sets of cells and UEs with active DL and UL transmissions, respectively. Hence, the DL received signal at the  $k^{\text{th}}$  UE, where  $k \in \mathcal{K}_{\text{dl}}$ ,  $c_k \in \mathfrak{B}_{\text{dl}}$ , is given by

$$\mathbf{y}_{k,c_k}^{\text{dl}} = \underbrace{\mathbf{H}_{k,c_k}^{\text{dl}} \mathbf{v}_k s_k}_{\text{Useful signal}} + \mathfrak{I}_k^{\text{dl}} + \mathbf{n}_k^{\text{dl}}, \quad (1)$$

where  $\mathbf{H}_{k,c_k}^{\text{dl}} \in \mathcal{C}^{M_r \times N_t}$  is the DL spatial channel from the cell serving the  $k^{\text{th}}$  UE, to the  $k^{\text{th}}$  UE,  $\mathbf{v}_k \in \mathcal{C}^{N_t \times 1}$ , and  $s_k$  are the single-stream pre-coding vector at the  $c_k^{\text{th}}$  cell, and data symbol of the  $k^{\text{th}}$  UE, respectively.  $\mathbf{n}_k^{\text{dl}}$  is the additive white Gaussian noise, while  $\mathfrak{I}_k^{\text{dl}}$  denotes the total interference seen at the  $k^{\text{th}}$  UE receiver end. Then,  $\mathfrak{I}_k^{\text{dl}}$  is expressed by

$$\mathfrak{I}_k^{\text{dl}} = \begin{cases} \sum_{i \in \mathcal{K}_{\text{dl}} \setminus k} \mathbf{H}_{k,c_i}^{\text{dl}} \mathbf{v}_i s_i, & \text{Aligned-TDD} \\ \underbrace{\sum_{i \in \mathcal{K}_{\text{dl}} \setminus k} \mathbf{H}_{k,c_i}^{\text{dl}} \mathbf{v}_i s_i}_{\text{DL-to-DL interference}} + \underbrace{\sum_{j \in \mathcal{K}_{\text{ul}}} \mathbf{G}_{k,j} \mathbf{w}_j s_j}_{\text{UL-to-DL interference}}, & \text{Flexible-TDD} \end{cases}, \quad (2)$$

where  $\mathbf{w}_j \in \mathcal{C}^{M_r \times 1}$  is the pre-coding vector at the  $j^{\text{th}}$  UE, and  $\mathbf{G}_{k,j} \in \mathcal{C}^{M_r \times M_r}$  is the the cross-link channel between the  $k^{\text{th}}$  and  $j^{\text{th}}$  UEs. Similarly, the received UL signal at the  $c_k^{\text{th}}$  cell, where  $c_k \in \mathfrak{B}_{\text{ul}}$  from  $k \in \mathcal{K}_{\text{ul}}$ , is given as

$$\mathbf{y}_{c_k,k}^{\text{ul}} = \underbrace{\mathbf{H}_{c_k,k}^{\text{ul}} \mathbf{w}_k s_k}_{\text{Useful signal}} + \mathfrak{I}_{c_k}^{\text{ul}} + \mathbf{n}_{c_k}^{\text{ul}}, \quad (3)$$

with the total UL interference  $\mathfrak{I}_{c_k}^{\text{ul}}$  calculated by

$$\mathfrak{I}_{c_k}^{\text{ul}} = \begin{cases} \sum_{j \in \mathcal{K}_{\text{ul}} \setminus k} \mathbf{H}_{c_k,j}^{\text{ul}} \mathbf{w}_j s_j, & \text{Aligned-TDD} \\ \underbrace{\sum_{j \in \mathcal{K}_{\text{ul}} \setminus k} \mathbf{H}_{c_k,j}^{\text{ul}} \mathbf{w}_j s_j}_{\text{UL-to-UL interference}} + \underbrace{\sum_{i \in \mathcal{K}_{\text{dl}}} \mathbf{Q}_{c_k,c_i} \mathbf{v}_i s_i}_{\text{DL-to-UL interference}}, & \text{Flexible-TDD} \end{cases}, \quad (4)$$

where  $\mathbf{Q}_{c_k,c_i} \in \mathcal{C}^{N_t \times N_t}$  is the cross-link channel between the cells serving the  $k^{\text{th}}$  and  $i^{\text{th}}$  UEs,  $k \in \mathcal{K}_{\text{ul}}$  and  $i \in \mathcal{K}_{\text{dl}}$ , and it is measured by orchestrating inter-BS coordinated sounding measurements [10]. Accordingly, the achievable post-processing signal-to-interference (SIR) ratio in the DL direction  $\gamma_k^{\text{dl}}$  and UL direction  $\gamma_{c_k}^{\text{ul}}$  are given by

$$\gamma_k^{\text{dl}} = \frac{\left\| (\mathbf{u}_k^{\text{dl}})^{\text{H}} \mathbf{H}_{k,c_k}^{\text{dl}} \mathbf{v}_k \right\|^2}{\sum_{i \in \mathcal{K}_{\text{dl}} \setminus k} \left\| (\mathbf{u}_k^{\text{dl}})^{\text{H}} \mathbf{H}_{k,c_i}^{\text{dl}} \mathbf{v}_i \right\|^2 + \sum_{j \in \mathcal{K}_{\text{ul}}} \left\| (\mathbf{u}_k^{\text{dl}})^{\text{H}} \mathbf{G}_{k,j} \mathbf{w}_j \right\|^2}, \quad (5)$$

$$\gamma_k^{\text{ul}} = \frac{\left\| (\mathbf{u}_k^{\text{ul}})^{\text{H}} \mathbf{H}_{c_k,k}^{\text{ul}} \mathbf{w}_k \right\|^2}{\sum_{j \in \mathcal{K}_{\text{ul}} \setminus k} \left\| (\mathbf{u}_k^{\text{ul}})^{\text{H}} \mathbf{H}_{c_k,j}^{\text{ul}} \mathbf{w}_j \right\|^2 + \sum_{i \in \mathcal{K}_{\text{dl}}} \left\| (\mathbf{u}_k^{\text{ul}})^{\text{H}} \mathbf{Q}_{c_k,c_i} \mathbf{v}_i \right\|^2}, \quad (6)$$

with  $\|\bullet\|^2$  as the second-norm, and  $\mathbf{u}_k^{\kappa} \in \mathcal{C}^{N_i/M_r \times 1}$ ,  $\mathcal{X}^{\kappa}$ ,  $\kappa \in \{\text{ul}, \text{dl}\}$ , is the linear minimum mean square error interference rejection combining (LMMSE-IRC) receiver [14], and  $(\bullet)^{\text{H}}$  denotes the Hermitian operation.

### III. PROBLEM FORMULATION

The URLLC outage performance is dominated by the achievable radio latency at the lower  $10^{-5}$  outage probability. This implies a stringent latency bound with a rare violation occurrence. Thus, in TDD deployments, due to the non-concurrent DL and UL transmission, the URLLC latency and reliability targets become highly susceptible to the number and placement of the DL  $d_c$  and UL  $u_c$  symbols during an RFC. Accordingly, our objective is to optimize the RFC selection in order to minimize the URLLC outage radio latency as

$$\left( \frac{d_c}{u_c} \right)^* \triangleq \left\{ \frac{d^i}{u^i} : \frac{d^i}{u^i} \in \mathfrak{T} \right\} \quad (7)$$

$$\text{s.t. } \arg \min_k (\varphi_{c,k}), \quad \forall k \in \mathcal{K}_{\text{ul/dl}},$$

where  $\mathfrak{T}$  is the set of all pre-defined possible RFC structures,  $\varphi_{c,k}$  is the one-way URLLC radio latency [4]. Accordingly, there is no feasible optimal solution of the DL  $d_c^{\text{opt}}$  and UL  $u_c^{\text{opt}}$  symbol structure to satisfy the UE-specific latency and reliability requirements. For instance, in multi-UE URLLC deployments, and due to the time-variant sporadic traffic arrivals, multiple UEs may request simultaneous opposite link directions. Thus, BSs instead adapt the RFC structure, on a best effort basis, to offer faster transmissions of the UEs with the worst latency performance while buffering other UEs. Adding the severe BS-BS CLI on top, victim UL packets most likely inflict several HARQ re-transmissions before a successful decoding, violating the UE-specific latency budget as well as dictating the RFC adaptation by pending packets rather than the new packet arrivals. Thus, to tackle this issue, we propose a semi-static coordinated RFC selection algorithm, which offers fully CLI-free transmissions while adapting the RFC selection to the varying URLLC latency statistics.

### IV. PROPOSED COORDINATION SCHEME

We propose a computationally-efficient RFC selection algorithm to offer a decent URLLC outage latency performance. First, cells estimate their average directional traffic size on a pre-defined periodicity. Then, a relative load metric is shared among the coordinating cells over the back-haul Xn-interface, i.e., multiple bits of feedback. Subsequently, a filtering window is applied on the reported traffic data-set, either to match

the average traffic volume per cluster, i.e., equal-priority windowing, or biasing the RFC adaptation towards individual cells, e.g., typically those with the worst traffic buffering performance. Then, a common RFC is estimated to match the filtered traffic volume, and accordingly, cells within the cluster adopt the same RFC until the next RFC update instant.

#### A. Cell-specific directional traffic tracking

Cells seek to select the RFCs which minimize the achievable average URLLC outage latency, according to (7). In multi-user URLLC networks, there may exist several active UEs with simultaneous UL and DL transmission requests, respectively, and hence, cross-directional target latency conflict is exhibited.

For the considered URLLC use cases, the incoming traffic is only allowed to be buffered for a short time-duration before being transmitted. Otherwise, the URLLC latency constraint is violated. We can therefore observe the strong correlation between the amount of buffered data, i.e., queuing of data payloads, and the experienced latency. Selecting the RFC that offers the best URLLC outage performance is therefore translated to selecting the RFC which minimizes the DL and UL buffering. As the offered traffic increases, buffering is obviously unavoidable, thus, the best feasible solution from the RFC selection point of view is to ensure that the traffic buffering of the two link directions is balanced.

Accordingly, at the  $\varrho^{\text{th}}$  slot of the radio frame,  $\varrho = 1, 2, \dots, \rho$ , with  $\rho$  as the number of slots per radio frame, the  $c^{\text{th}}$  cell calculates the aggregated DL  $Z_c^{\text{dl}}(\varrho)$  and UL  $Z_c^{\text{ul}}(\varrho)$  buffered traffic size, respectively. Specifically, the UL traffic volume is identified at the cell side from the UE scheduling requests, and the associated buffer status reports. Thus, the normalized traffic ratio  $\mu_c(\varrho)$  is defined as

$$\mu_c(\varrho) = \frac{Z_c^{\text{dl}}(\varrho)}{Z_c^{\text{dl}}(\varrho) + Z_c^{\text{ul}}(\varrho)}. \quad (8)$$

Then, the instantaneous traffic ratios  $\mu_c(\varrho)$  are linearly averaged across each frame duration as expressed by

$$\bar{\mu}_c = \frac{1}{\rho} \sum_{\varrho=1}^{\rho} \mu_c(\varrho), \quad (9)$$

where  $\bar{\mu}_c$  implies the averaged traffic ratio of the  $c^{\text{th}}$  cell. In case there are neither DL and UL new packet arrivals or buffered traffic, BSs fall-back to a default RFC structure until the next update instant. The larger the  $\bar{\mu}_c$ , e.g.,  $\sim 1$ , the larger the buffered DL traffic compared to the corresponding UL traffic volume. For instance, with  $\bar{\mu}_c = 0.9$ , the DL traffic volume is 9x the respective UL volume. Finally, per every RFC adaptation period, neighboring cells exchange the measured  $\bar{\mu}_c$  over the Xn-interface.

#### B. Traffic filtering and common RFC selection

As the URLLC outage performance is mainly dominated by the cells of the worst latency and reliability performance, we apply a window filtering to dynamically control the URLLC latency tail distribution, i.e., outage latency. Thus, based on the exchange of  $\bar{\mu}_c$ , the most problematic cells are first identified

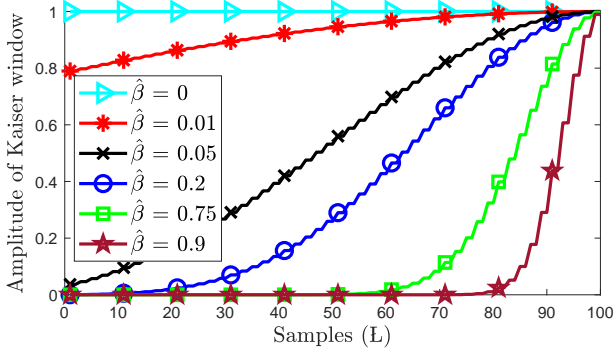


Fig. 2. Mirrored Kaiser window with  $\hat{\beta}$ .

as those inflicting the largest or smallest  $\bar{\mu}_c$ , i.e., having too large DL or UL buffered traffic volume, which implies the RFC adaptation is not properly configured for those victim cells. In this regard, cells calculate the absolute linear distance of the reported  $\bar{\mu}_c$  data-set towards its mean value  $d$ , i.e.,  $d = 0.5$ , and then, sort them in an descending order in terms of their respective absolute linear distance, as given by

$$\Psi = \underset{x^{(a)}, y^{(b)}; a > b}{\text{Sort}} \left[ \bar{\mu}_1^{(|\bar{\mu}_1 - d|)}, \bar{\mu}_2^{(|\bar{\mu}_2 - d|)}, \dots, \bar{\mu}_C^{(|\bar{\mu}_C - d|)} \right]. \quad (10)$$

The ordered traffic data-set  $\Psi = [\psi_1, \psi_2, \dots, \psi_C]$  is then filtered using a spatial window. In this work, we consider the Kaiser window  $w[l]$ , due to its flexible response tunability, and is given in the discrete domain as

$$w[l] = \frac{I_0 \left[ \beta \sqrt{1 - \left( \frac{2l}{L} - 1 \right)^2} \right]}{I_0[\beta]}, \quad 0 \leq l \leq L \quad (11)$$

with  $I_0$  as the zeroth-order modified Bessel function of the first kind,  $\beta$  is the window shaping factor, and  $L + 1$  denotes the window length. As depicted by Fig. 2, the mirrored Kaiser window amplitude is shown for various normalized shaping factors  $\hat{\beta} = \frac{\beta}{\beta_{\max}}$ , with  $\beta_{\max} = 100$  and  $L = 100$ . The larger the  $\hat{\beta}$  factor, the more selective the Kaiser window. For instance, with  $\hat{\beta} = 0$ , the mirrored Kaiser window approaches a conventional band pass filter, i.e., all cells are equally prioritized; although, with a larger  $\hat{\beta} = 0.9$ , the window becomes highly selective over a subset of the sample space, i.e., certain cells are highly prioritized.

Accordingly, the Kaiser window coefficients are applied in a descending order on the sorted data-set  $\Psi$ , as

$$\Theta = \frac{\psi_1 w[0] + \psi_2 w[1] + \dots + \psi_C w[L]}{w[0] + w[1] + \dots + w[L]}, \quad L = C - 1, \quad (12)$$

where  $\Theta$  is the filtered traffic ratio per the entire cluster, with  $w[0] > w[1] > \dots > w[L]$ . Based on the calculated  $\Theta$ , a common RFC is selected and adopted by all cells within the cluster until the next RFC update instant. For example, with an estimated  $\Theta = 0.2$ , a common RFC of  $d_c/u_c \simeq \frac{1}{4}$  is adopted across all cells, with the DL/UL symbol placement configured according to the strategy presented in Section II.

Table I: Simulation parameters.

Parameter	Value
Environment	3GPP-UMA, one cluster, 21 cells
UL/DL channel bandwidth	10 MHz, SCS = 30 KHz, TDD
Carrier frequency	3.5 GHz
TDD mode	Synchronized
Antenna setup	$N_t = 8, M_r = 2$
Average user load per cell	$K^{\text{dl}} = K^{\text{ul}} = 10$
TTI duration	4-OFDM symbols
Traffic model	FTP3, $f^{\text{dl}} = f^{\text{ul}} = 400$ bits $\lambda^{\text{dl}} = 125$ , and 375 pkts/sec $\lambda^{\text{ul}} = 125$ , and 375 pkts/sec
Offered load ratio	DL:UL = 1:1
Processing time	Preparation delay: 3-OFDM symbols PDSCH decoding: 4.5-OFDM symbols PUSCH decoding: 5.5-OFDM symbols
RFC update periodicity	10 ms (radio frame)
UL/DL receiver	LMMSE-IRC
Link adaptation	Adaptive modulation and coding
HARQ configuration	asynchronous with Chase Combining

### C. Comparison to the state-of-the-art TDD studies

We compare the performance of the proposed solution against the state-of-the-art TDD solutions in the recent literature as follows:

**Static-TDD (sTDD):** a pre-defined RFC is globally configured for all cells across the entire network, where it matches the average network traffic demand. Herein, we define  $\alpha$  as the normalized RFC mismatch error, where  $\alpha = 0$  implies the global RFC is selected to perfectly match the average network traffic statistics and  $\alpha = 0.35$  denotes 35% symbol mismatch of the configured RFC against the actual average offered traffic load. sTDD deployments offer CLI-free conditions; though, with a limited cross-cell traffic adaptation flexibility.

**Dynamic TDD (dTDD):** a fully flexible TDD operation is assumed, where at each RFC update period, each cell independently adopts the RFC which best meets its individual traffic demand. We consider two scenarios of the dTDD deployments as: (a) a dTDD setting with an optimal CLI cancellation (dTDD-CLI-free) [9], where the BS-BS and UE-UE are perfectly suppressed using full packet exchange over both the back-haul and radio interfaces, and (b) a dTDD deployment with CLI coexistence (dTDD-CLI).

## V. PERFORMANCE EVALUATION

We assess the performance of the proposed solution using extensive system-level simulations, with a high degree of realism. The major simulation settings are listed in Table I, where the main assumptions of the 3GPP release-15 for TDD deployments are adopted. During every RFC update periodicity, cells estimate their buffered traffic ratio, according to (8), and hence, share it among the cluster in order to estimate a common RFC. Thus, during each TTI, DL and UL UEs are dynamically multiplexed using OFDMA based on the PF metric. The signal-to-interference-noise-ratio (SINR) points of the individual SCs are calculated by the LMMSE-IRC receiver, and combined into an effective SINR level using the exponential SNR mapping [15]. Finally, we adopt a dynamic link adaptation, i.e., adaptive modulation and coding selection, and asynchronous HARQ Chase combining, where

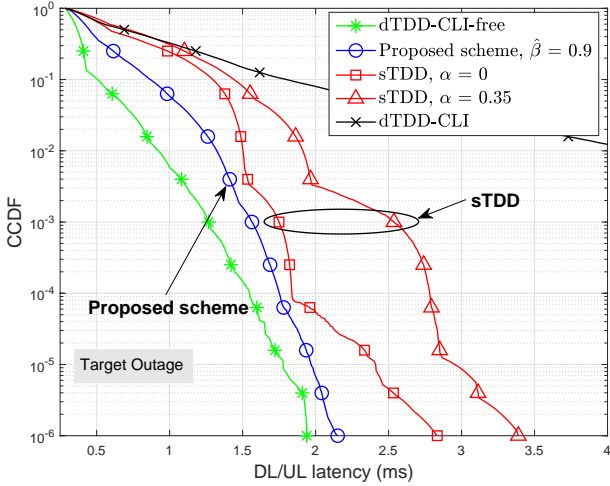


Fig. 3. Achievable URLLC outage latency of proposed scheme, sTDD, and dTDD, with  $\Omega = 1$  Mbps.

the HARQ re-transmissions are dynamically scheduled, and are always prioritized over new transmissions.

Fig. 3 depicts the complementary cumulative distributive function (CCDF) of the DL/UL combined URLLC one-way radio latency in ms, of the proposed scheme, sTDD, and dTDD, respectively, for  $\Omega = 1$  Mbps. Looking at the achievable latency at the  $10^{-5}$  probability level, i.e., URLLC outage latency, the proposed solution clearly offers a decent URLLC outage performance, approaching the optimal dTDD-CLI-free. It achieves  $\sim 20\%$  and  $\sim 40\%$  reduction of the URLLC outage latency, compared to the sTDD with a perfect RFC match, i.e.,  $\alpha = 0$  and non-perfect RFC match, i.e.,  $\alpha = 0.35$ , respectively. However, the proposed solution inflicts  $\sim 10\%$  URLLC outage latency degradation against the ideal dTDD-CLI-free; although, this comes with a significantly lower control signaling overhead size. In that sense, the proposed solution relaxes one of the most challenging requirements of the conventional sTDD schemes, as it does not require a pre-configured RFC, while still preserving fully CLI-free transmissions with a semi-static traffic adaptation.

Furthermore, the dTDD-CLI-free achieves the best URLLC outage latency, i.e.,  $\sim 1.78$  ms, due to the fully flexible, i.e., cell-wise, RFC adaptation to the individual sporadic traffic arrivals. Though, it comes with the assumption of optimal CLI-free conditions. The dTDD-CLI scheme exhibits an outage latency saturation, since the URLLC radio performance becomes dictated by the aggressive BS-BS CLI, instead of the RFC adaptation, leading to the consumption of the maximum HARQ attempts before UL packets are either dropped or successfully received after the Chase combining HARQ process.

Fig. 4 shows the CCDF of the URLLC latency of the proposed solution, with different  $\hat{\beta}$  settings, and  $\Omega = 3$  Mbps. As can be noticed, with  $\hat{\beta} = 0.9$ , the tail of the URLLC latency distribution becomes more narrower, since the cells with the worst traffic buffering performance are highly prioritized in selecting the upcoming RFCs. With a smaller  $\hat{\beta}$  factor, the reported traffic statistics of the coordinating cells are equally prioritized, leading to a wider latency tail distribution. That is

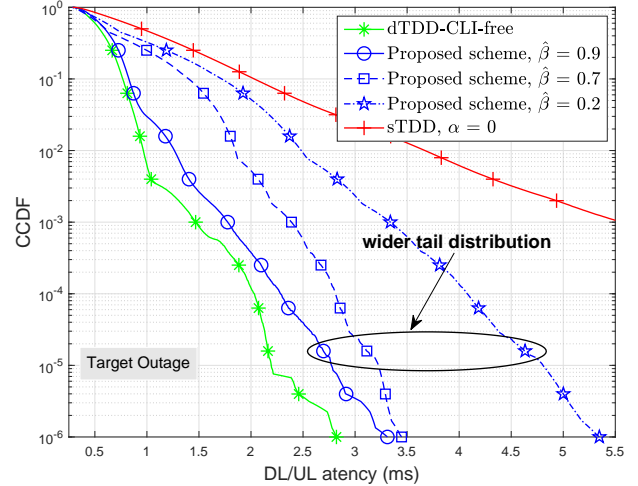
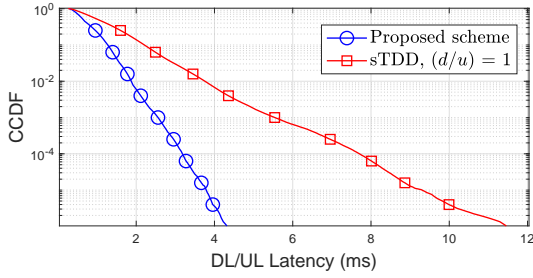


Fig. 4. Achievable URLLC outage latency of proposed scheme, with  $\hat{\beta}$  and  $\Omega = 3$  Mbps.

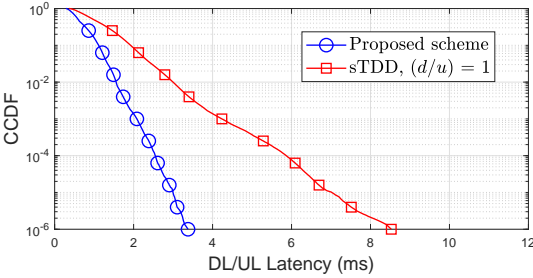
$\sim +54\%$  increase in the URLLC outage latency with  $\hat{\beta} = 0.2$ , compared to the case with  $\hat{\beta} = 0.9$ . This consolidates the fact that the URLLC outage latency is dictated by the cells of the worst buffering imbalance. Hence, those should be given a higher priority when deciding the upcoming RFCs, in order to rapidly recover their respective outage targets.

Looking at the URLLC outage performance with different  $\Omega^{\text{dl}}/\Omega^{\text{ul}}$  ratios, Fig. 5 depicts the CCDF of the URLLC radio latency, under the proposed and the sTDD schemes, respectively, where the latter is configured with  $d_c/u_c = 1$ , for  $\Omega^{\text{dl}}/\Omega^{\text{ul}} = 3 : 1$  and  $1 : 3$ . The proposed solution offers a sufficient frame adaptation against the variable offered traffic ratio  $\Omega^{\text{dl}}/\Omega^{\text{ul}}$ , resulting in a decent URLLC outage latency, i.e., 3.8 ms for  $\Omega^{\text{dl}}/\Omega^{\text{ul}} = 3 : 1$  and 2.9 ms for  $\Omega^{\text{dl}}/\Omega^{\text{ul}} = 1 : 3$ , respectively. The sTDD scheme clearly exhibits a significant outage latency increase due to the mismatch between the predefined  $d_c/u_c = 1$  and the offered traffic ratio  $\Omega^{\text{dl}}/\Omega^{\text{ul}}$ , e.g., proposed solution offers  $\sim 82\%$  outage latency reduction compared to the sTDD scheme. Accordingly, the proposed solution eliminates the rigid requirement of pre-configuring a global RFC while offering a semi-static RFC adaptation to the varying offered traffic.

Finally, Fig. 6 depicts a comparison of the achievable combined DL/UL outage latency with various offered load levels, in reference to the dTDD-CLI-free scheme. At the very low offered region  $\Omega = 0.25$  Mbps, with an average of a single active UE per cell, the traffic demand becomes highly variant among neighboring cells. Accordingly, the URLLC outage performance is dominated by how fast the cells adapt their individual RFCs to the sporadic traffic arrivals. Thus, both the proposed solution and sTDD schemes inflict a considerable outage latency degradation, compared to the optimal dTDD-CLI-free, i.e.,  $+29\%$  and  $+63\%$  latency increase. However, the proposed scheme outperforms the corresponding sTDD by 35% outage latency reduction gain. This is mainly attributed to the semi-static cross-cell RFC adaptation of the proposed solution. Thus, unlike sTDD, cells with accumulating traffic



(a) DL-heavy ( $\Omega^{\text{dl}} : \Omega^{\text{ul}} = 3 : 1$ )



(b) UL-heavy ( $\Omega^{\text{dl}} : \Omega^{\text{ul}} = 1 : 3$ )

Fig. 5. Comparison of the URLLC latency performance with various DL and UL traffic ratios,  $\Omega = 3$  Mbps.

size are given higher priority in selecting the RFCs. Over the high load region  $\Omega = 5$  Mbps, similar conclusions are observed; although, with less outage latency relative degradation compared to the optimal dTDD-CLI-free, since in this case, the URLLC outage performance is mainly dictated by the scheduling queuing delay rather than the flexibility of the RFC adaptation operation.

## VI. CONCLUDING REMARKS

A semi-static radio frame configuration (RFC) selection algorithm has been proposed for 5G TDD macro deployments. Proposed solution incorporates a simple inter-cell signaling exchange procedure of the relative traffic statistics, in order to estimate a common RFC of each cluster, which matches the time-variant and cell-specific traffic demand. Compared to the state-of-the-art TDD literature, the proposed solution demonstrates an attractive trade-off between the achievable URLLC outage performance and the signaling overhead size. It achieves  $\sim 40\%$  reduction of the URLLC outage latency, compared to the ideal static-TDD deployment, while approaching the optimal dynamic-TDD bound; though, with a significantly lower signaling overhead size.

The main insights brought by this paper are as follows: (a) within macro 5G new radio deployments, the cross-cell traffic statistics are of a low time-variance due to the sufficiently large number of active connected users, (b) accordingly, relaxing the requirements of fast traffic adaptation for the sake of controlling the critical cross-link interference (CLI) is of a more significance, and (c) the proposed solution offers a flexible and semi-static RFC adaptation to the sporadic cross-cell traffic demand, with fully CLI-free conditions and limited signaling overhead.

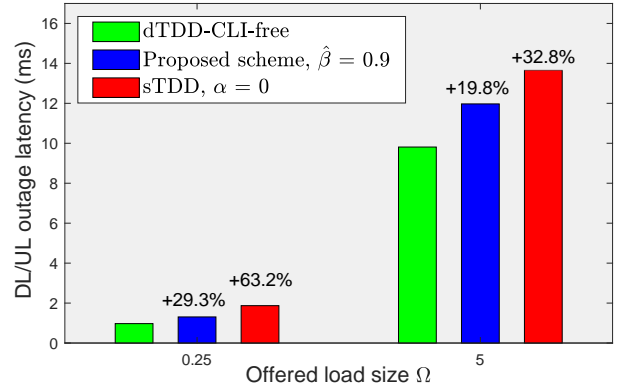


Fig. 6. Comparison of the URLLC latency performance with various offered load levels  $\Omega$ .

## VII. ACKNOWLEDGMENTS

This work is partly funded by the Innovation Fund Denmark – File: 7038-00009B. The authors would like to acknowledge the contributions of their colleagues in the project, although the views expressed in this contribution are those of the authors and do not necessarily represent the project.

## REFERENCES

- [1] IMT vision – “Framework and overall objectives of the future development of IMT for 2020 and beyond”, international telecommunication union (ITU), ITU-R M.2083-0, Feb. 2015.
- [2] Service requirements for the 5G system; Stage-1 (Release 16), 3GPP, TS 22.261, V16.6.0, Dec. 2018.
- [3] J. Lee et al., “Spectrum for 5G: global status, challenges, and enabling techs,” *IEEE Commun. Mag.*, vol. 56, no. 3, pp. 12-18, March 2018.
- [4] Ali A. Esswie, and K.I. Pedersen, “On the ultra-reliable and low-latency communications in flexible TDD/FDD 5G networks,” in *Proc. IEEE CCNC*, Las Vegas, 2020.
- [5] *5G; NR; Physical layer procedures for control*; (Release 15), 3GPP, TS 38.213, V15.3.0, Oct. 2018.
- [6] *Cross link interference handling and remote interference management (RIM) for NR*; (Release 16); 3GPP, TR 38.828, V16.0.0, June 2019.
- [7] A. Łukowa and V. Venkatasubramanian, “Performance of interference cancellation in flexible TDD systems using coordinated muting, scheduling and rate allocation,” in *Proc. IEEE WCNC*, Doha, 2016, pp. 1-7.
- [8] Z. Huo, N. Ma and B. Liu, “Joint user scheduling and transceiver design for cross-link interference suppression in MU-MIMO dynamic TDD systems,” in *Proc. IEEE ICC*, Chengdu, 2017, pp. 962-967.
- [9] R1-1701146, *Dynamic TDD interference mitigation concepts in NR*, Nokia, Alcatel-Lucent Shanghai Bell, 3GPP RAN1 #88, Feb. 2017.
- [10] Ali A. Esswie, and K.I. Pedersen, “Cross link interference suppression by orthogonal projector in 5G dynamic-TDD URLLC systems,” *Submitted to IEEE Commun. Lett.*, 2019.
- [11] Ali A. Esswie, K.I. Pedersen, and P. Mogensen, “Quasi-dynamic frame coordination for ultra-reliability and low-latency in 5G TDD systems,” in *Proc. IEEE ICC*, Shanghai, China, 2019, pp. 1-6.
- [12] J. W. Lee, C. G. Kang and M. J. Rim, “SINR-ordered cross link interference control scheme for dynamic TDD in 5G system,” in *Proc. IEEE ICOIN*, Chiang Mai, 2018, pp. 359-361.
- [13] A. A. Esswie and K. I. Pedersen, “Inter-cell radio frame coordination scheme based on sliding codebook for 5G TDD systems,” in *Proc. IEEE VTC*, Kuala Lumpur, Malaysia, 2019, pp. 1-6.
- [14] Tavares, F.M.L.; Berardinelli, G.; Mahmood, N.H.; Sorensen, T.B.; Mogensen, P., “On the potential of interference rejection combining in B4G networks,” in *Proc. IEEE VTC*, Las Vegas, NV, 2013, pp. 1-5.
- [15] S. N. Donthi and N. B. Mehta, “An accurate model for EESM and its application to analysis of CQI feedback schemes and scheduling in LTE,” *IEEE Trans. Wireless Commun.*, vol. 10, no. 10, pp. 3436-3448, Oct. 2011.